Signaling and Cross-talk by C5a and UDP in Macrophages Selectively Use PLCβ3 to Regulate Intracellular Free Calcium*[S]

Tamara I. A. Roach[‡1,2], Robert A. Rebres[‡1,3], Iain D. C. Fraser[§], Dianne L. DeCamp[¶], Keng-Mean Lin[¶], Paul C. Sternweis[¶], Mel I. Simon[§], and William E. Seaman[‖4]

From the Alliance for Cellular Signaling, [‡]Northern California Institute for Research and Education and the [‖]University of California, Veterans Affairs Medical Center, San Francisco, California 94121, the [§]Division of Biology, California Institute of Technology, Pasadena, California 91125, and the [¶]University of Texas Southwestern Medical Center, Dallas, Texas 75390

Studies in fibroblasts, neurons, and platelets have demonstrated the integration of signals from different G protein-coupled receptors (GPCRs) in raising intracellular free Ca^{2+}. To study signal integration in macrophages, we screened RAW264.7 cells and bone marrow-derived macrophages (BMDM) for their Ca^{2+} response to GPCR ligands. We found a synergistic response to complement component 5a (C5a) in combination with uridine 5′-diphosphate (UDP), platelet activating factor (PAF), or lysophosphatidic acid (LPA). The C5a response was $G\alpha_i$-dependent, whereas the UDP, PAF, and LPA responses were $G\alpha_q$-dependent. Synergy between C5a and UDP, mediated by the C5a and P2Y6 receptors, required dual receptor occupancy, and affected the initial release of Ca^{2+} from intracellular stores as well as sustained Ca^{2+} levels. C5a and UDP synergized in generating inositol 1,4,5-trisphosphate, suggesting synergy in activating phospholipase C (PLC) **β**. Macrophages expressed transcripts for three PLCβ isoforms (PLCβ2, PLCβ3, and PLCβ4), but GPCR ligands selectively used these isoforms in Ca^{2+} signaling. C5a predominantly used PLCβ3, whereas UDP used PLCβ3 but also PLCβ4. Neither ligand required PLCβ2. Synergy between C5a and UDP likewise depended primarily on PLCβ3. Importantly, the Ca^{2+} signaling deficiency observed in PLCβ3-deficient BMDM was reversed by re-constitution with PLCβ3. Neither phosphatidylinositol (PI) 3-kinase nor protein kinase C was required for synergy. In contrast to Ca^{2+}, PI 3-kinase activation by C5a was inhibited by UDP, as was macropinocytosis, which depends on PI 3-kinase. PLCβ3 may thus provide a selective target for inhibiting Ca^{2+} responses to mediators of inflammation, including C5a, UDP, PAF, and LPA.

Calcium is an important messenger involved in the regulation of multiple cellular processes, and levels of intracellular free calcium ($[Ca^{2+}]_i$)[5] are precisely regulated (1–3). Increases in intracellular $[Ca^{2+}]_i$ are initiated by the phospholipase C (PLC) family of enzymes, which hydrolyze membrane-associated phosphatidylinositol 4,5-diphosphate (PIP_2) to produce inositol-1,4,5-trisphosphate (IP_3) and diacylglycerol (4). IP_3 triggers the release of Ca^{2+} from stores in the endoplasmic reticulum, whereas diacylglycerol activates members of the protein kinase C (PKC) family. Following activation of stored Ca^{2+} by IP_3, influx of extracellular Ca^{2+} across the plasma membrane may further contribute to an increase in $[Ca^{2+}]_i$, which is regulated by several Ca^{2+} pumps and buffers (1). The net level and duration of these Ca^{2+} signals regulate cellular responses, including transcription, apoptosis, endocytosis, chemotaxis, and metabolism (3).

Simultaneous stimulation of two GPCRs coupled to different $G\alpha$ subunits, often $G\alpha_i$ or $G\alpha_s$ in combination with $G\alpha_q$, has been shown to yield synergistic Ca^{2+} responses in several model systems (reviewed in Ref. 5). Limited studies have demonstrated this synergy in primary cells, including neurons and platelets, but the mechanisms of synergy vary and are not well defined (6, 7).

Synergistic Ca^{2+} responses resulting from heterologous GPCR ligation have been little studied in macrophages, where members of the GPCR superfamily can stimulate an increase in $[Ca^{2+}]_i$ by activating members of the PLCβ family (4). As part of a systematic screen of RAW264.7 macrophage cells, C5a and UDP demonstrated synergy in producing a rise in $[Ca^{2+}]_i$ (8). C5a is an important inflammatory mediator for macrophages and UDP, which is released following cell damage, is also present at sites of injury or infection (9, 10). Both ligands signal through GPCRs; C5a signals through C5aR (11), and UDP signals through P2Y6 receptors (12). To examine GPCR cross-talk by these ligands in mouse macrophages we studied both

---

[S] The on-line version of this article (available at http://www.jbc.org) contains supplemental Figs. S1–S4.

[1] Both authors contributed equally to this manuscript.

[2] To whom correspondence may be addressed: VAMC 111R, 4150 Clement St., San Francisco, CA 94121. Tel.: 415-750-2104; Fax: 415-750-6920; E-mail: Tamara.Roach@ucsf.edu.

[3] To whom correspondence may be addressed. E-mail: Robert.Rebres@ucsf.edu.

[4] To whom correspondence may be addressed. E-mail: bseaman@medicine.ucsf.edu.

[5] The abbreviations used are: $[Ca^{2+}]_i$, intracellular free calcium; BMDM, bone marrow-derived macrophages; C5a, complement component 5a; GPCR, G protein-coupled receptor; GRK, G protein-coupled receptor kinase; IP_3, inositol 1,4,5-trisphosphate; LPA, lysophosphatidic acid; PAF, platelet activating factor; PIP_2, phosphatidylinositol 4,5-diphosphate; PKC, protein kinase C; PI3K, phosphatidylinositol 3-kinase; PLC, phospholipase C; PTX, pertussis toxin; ERK, extracellular signal-regulated kinase; WT, wild type; YFP, yellow fluorescent protein; RNAi, RNA interfering; shRNA, short hairpin RNA.

RAW264.7 cells and primary bone marrow-derived macrophages (BMDMs).

Our studies show that signals generated by C5a and UDP, acting through $G\alpha_i$- and $G\alpha_q$-coupled pathways, respectively, converge at the level of PLCβ, and that these ligands, both individually and in concert, selectively use one PLCβ isoform, PLCβ3, to activate the production of IP_3 and the consequent release of Ca^{2+} from intracellular stores.

EXPERIMENTAL PROCEDURES

Reagents—UDP, UTP, LPA, platelet activating factor (PAF), human C5a, and fluorescein isothiocyanate-dextran were from Sigma. Mouse IgG_{2a} was from BD Pharmaceuticals. $F(ab')_2$ fragment of goat anti-mouse IgG was from Jackson ImmunoResearch Inc. Anti-PLCβ3 was from P. Sternweis, University of Texas Southwestern Medical Center. Anti-P-Akt and anti-P-ERK were from Cell Signaling Technologies. Fura2 was from Molecular Probes. Ionomycin, thapsigargin, pertussis toxin, LY294002, wortmannin, Calphostin C, staurosporine, U-73122, and U-73343 were from Calbiochem. Additional detailed protocols for reagents, procedures, and solutions are available on the internet and are referenced according to protocol number (*e.g.* PP00000226).

Culture of RAW264.7 Cells—This is described in protocol PP00000226. Following lentiviral infection, positive transductants were selected by antibiotic resistance conferred by the particular viral construct used (PP00000206). These included puromycin (2 μg ml), G418 (100–500 μg/ml), hygromycin (50 μg/ml), and zeocin (100 μg/ml). Detailed specifications for each medium are available on request.

Mice and Culture of BMDM—Mice genetically deficient in $G\alpha_q$, $G\alpha_{11}$, PLCβ3, PLCβ4, or PLCβ2 were previously described (13–19). All strains were on the C57BL/6 background except PLCβ2-deficient mice, which were on 129SV. Genetically deficient and corresponding wild-type (WT) strains were bred and housed under approved animal protocols. For BMDM culture femurs and tibias were removed from sex- and age-matched mice (4–20 weeks of age, matched ± 4 weeks) (PP0000017200). Briefly, marrow was flushed from bones, erythrocytes were lysed, and the white cells were seeded in non-tissue culture Petri dishes for selection by growth and adhesion. After 6 days, over 99% of the surviving cells were macrophages, and these cells were maintained for up to 35 days in culture. Cells were cultured overnight in tissue culture plates prior to use in assays.

Lentivirus-mediated RNAi—Lentivirus was produced with a combination of three plasmids: (i) pCMVΔR8.91 packaging plasmid, (ii) pMD.G envelope plasmid (20, 21), and (iii) a lentiviral vector plasmid. The packaging and envelope plasmids were generously provided by D. Trono, Geneva. The lentiviral vector plasmids contained shRNA sequences expressed under RNA polymerase III promoters (U6 or H1) upstream of a Ubi-C promoter driving bicistronic expression of either enhanced green fluorescent protein or an hCD4 marker, followed by a resistance gene for either puromycin or hygromycin (22). Transfection of the 3 plasmids into 293T cells utilized Lipofectamine 2000 (Invitrogen) and 20 μg of total DNA in a ratio of 4:3:2 for vector, packaging, and envelope plasmids, respectively

(PP00000200). Two days post-transfection, lentivirus was concentrated by using Centricon microfiltration tubes (PP00000202). Macrophages were infected at a multiplicity of infection of ∼10 in the presence of Polybrene at 4 μg/ml (PP00000215) (22). shRNAs targeting murine PLCβ2, PLCβ3, and PLCβ4 employed the sequences GAA CAG AAG TTA CGT TGT C; GCA GCG AGA TGA TTT GAT T; and ACG CGA TTG AGT TTG TAA ATT A, respectively.

*Retrovirus-mediated Transduction of Macrophages with PLCβ*—pFB-neo vectors carrying YFP-tagged murine PLCβ3 or YFP-FLAG epitope were transfected into the PlatE packaging line (23) to produce ecotropic retroviruses for transduction of day 2 cultures of bone marrow cells, which were differentiated into BMDM as described above.

Population Calcium Assays—Ca^{2+} responses were measured by monitoring the fluorescence of Fura2-loaded cells (PP00000211). Baseline readings were collected for 30–40 s. Calibration steps included additions of a Ca^{2+}-minimizing solution (PS00000607) and Fura2 Ca^{2+}-saturating solution (PS00000608) at the end of each recording, to allow calculation of $[Ca^{2+}]_i$ values according to the method of Grynkiewicz *et al.* (24), assuming a cytoplasmic K_d of 250 nM for Fura2. Ca^{2+} signals during the response period were quantified by features as indicated, including the peak offset response (difference between baseline Ca^{2+} level and the maximal Ca^{2+} level observed, reported in nanomolar) and an integrated response (integrated Ca^{2+} level above the average baseline over the indicated time period, reported in nanomolar × seconds).

Single-cell Calcium Assays—BMDM were plated in chambered coverglasses (Nunc, 8 wells/coverglass), cultured overnight, and loaded with Fura2-AM as described above. Video microscopy was performed on a Nikon TE-300 fluorescence microscope equipped with a Photometrics HQ2 camera, 37 °C stage incubator (Bionomics), Xe lamp (Sutter), and filter/shutter/dichoric controllers (Sutter and Conix). Simple PCI software was used to control collection parameters and extract fluorescence intensity data for individual cells.

IP_3 Assay—After cell culture overnight, cells were placed in serum-free medium containing, 0.01% bovine serum albumin. After 1 h, ligands were added and, after varied time periods, dishes were transferred to ice, the media aspirated, and the cells washed with cold phosphate-buffered saline. Cells were scraped into 125 μl of 5.4% perchloric acid solution and transferred to siliconized microcentrifuge tubes on ice. Samples were centrifuged at 14,000 × g for 15 min at 4 °C. 120 μl of supernatant was neutralized with 5 N KOH containing 60 mM HEPES, and the samples recentrifuged at 14,000 × g for 15 min at 4 °C. The IP_3 content of the final supernatant was assayed with an Amersham Biosciences IP_3 [³H] Biotrak assay kit. Results were reported as picomoles of IP_3 per 10⁶ cells.

SDS-PAGE and Western Blot Analysis of Phosphoproteins (Protocols PP00000168 and PP00000181)—Cells were stimulated under the same conditions used for the IP_3 assay. Then buffer was aspirated, the cells were scraped into Laemmli sample buffer, and the samples heated. SDS-PAGE gels were loaded with 20 μg of protein per lane, and Western blots were probed with anti-P-Akt, anti-P-ERK, and anti-Rho-GDI. Fluorescent
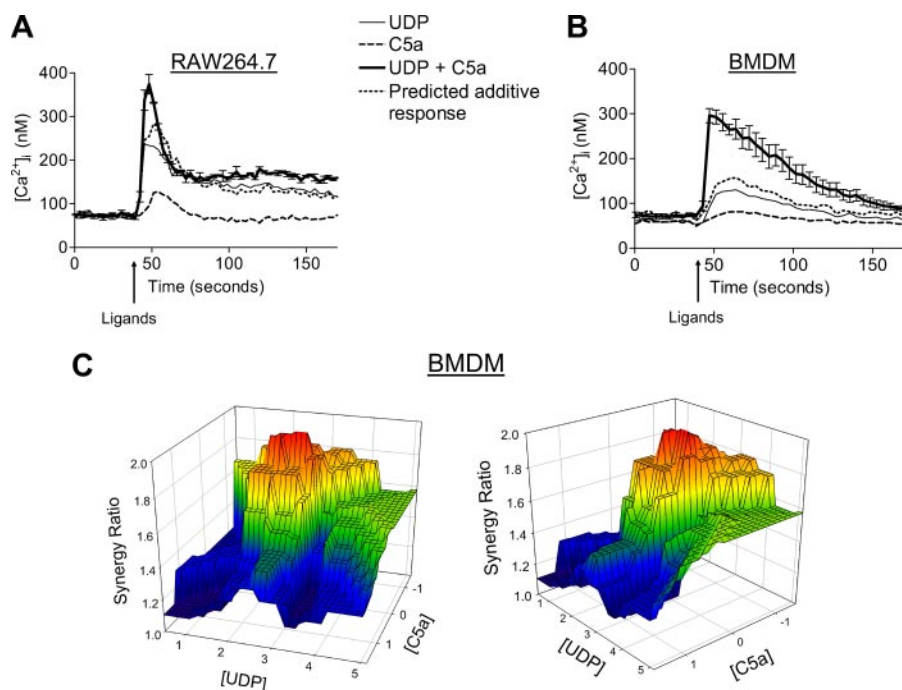
FIGURE 1. **UDP and C5a produce a synergistic Ca^{2+} response in macrophages.** Intracellular Ca^{2+} levels were calculated for Fura2-loaded adherent macrophage populations from kinetic assays in 96-well plates. After 40-s baseline readings, ligands were added and responses were monitored for 2.5 min. Each line in the graphs represents the average of three to four individual wells per assay and the error bars (S.E.) are shown for the dual ligand line in each graph. Synergy was evaluated by comparing the experimentally observed dual ligand responses to the predicted additive responses of the individual ligands. The dual ligand response was quantified as the ratio of the observed/predicted additive responses and the term "synergy ratio" was applied to the ratio of the peak offsets (PO = peak height − baseline). *A*, RAW264.7 cells were stimulated with UDP (2.5 μM), C5a (10 nM), or simultaneous UDP and C5a. Synergy ratio = 1.38. This is a representative experiment of *n* = 12 with similar results. *B*, BMDM were stimulated with UDP (500 nM), C5a (0.37 nM), or simultaneous UDP and C5a. Synergy ratio = 2.62. This is a representative experiment of >25 with similar results. *C*, dose response pattern for simultaneous UDP- and C5a-stimulated Ca^{2+} responses quantified by the synergy ratio. Ligand concentrations are expressed as log (nM). The optimal synergy ratio was at ~300 nM UDP + 0.3 nM C5a. The surface was interpolated from 84 individual experiments composed of 15 samples each.

signals, measured for P-Akt and P-ERK by using a phosphorimager, were normalized to Rho-GDI.

Macropinocytosis Assay—Macropinocytosis was assessed by measuring the cellular uptake of fluorescently labeled fluorescein isothiocyanate-dextran. In brief, BMDM cells were cultured overnight in non-tissue culture plates. Medium was replaced with Hanks' balanced salt solution with 1 mg/ml bovine serum albumin, pH 7.4. After 1 h ligands were added together with fluorescein isothiocyanate-dextran (150 kDa, Sigma, 1 mg/ml final concentration in well). Activity was stopped with cold medium. After washing, cells were harvested in phosphate-buffered saline with 5 mM EDTA and 5 mg/ml bovine serum albumin, and analyzed by flow cytometry (FACSCalibur, BD Biosciences) in 0.4% trypan blue solution (Sigma) to quench extracellular fluorescence. Ligand-stimulated activity was expressed as a ratio ("-fold stimulation") to baseline activity.

Statistical Analyses—The error bars in graphs depict the mean ± S.E. The statistical significance of each comparison was evaluated by performing Student's *t* tests for one-way analysis of variance, followed by Dunnett or individual *t* tests (with Bonferroni correction), or non-linear mixed effects modeling, as appropriate. The effects of RNAi on Ca^{2+} responses in RAW264.7 cells were analyzed by non-linear mixed effects

modeling because of the non-normal distribution of Ca^{2+} response features, and because of variation in responses between cell lines and assays. A *p* value of <0.05 was considered significant.

RESULTS

UDP and C5a Interact to Produce a Synergistic Calcium Response in Macrophages—As part of a large-scale screen, we observed a synergistic interaction between UDP and C5a for Ca^{2+} signaling (8). This response showed a faster rise time and an increased peak offset (peak response minus baseline) compared with the predicted additive response by the individual ligands (Fig. 1*A*). For the peak offset, the observed dual ligand response was increased by 1.5–2-fold over the predicted additive response. Integration of the response over the first 20 s yielded similar values. The ratio of observed/predicted values for such features of the response was referred to as the synergy ratio. BMDM showed a similar synergistic increase in the Ca^{2+} response, but the synergy ratio was much greater than in RAW264.7 cells (Fig. 1*B*).

For both cell types the optimal synergistic concentrations of each ligand were at or near the threshold for stimulation (Fig. 1*C* for BMDM, RAW264.7 data not shown). Synergy was nonetheless still observed at higher concentrations of both ligands, which fell within the linear portions of their dose-response curves. For RAW 264.7 cells, optimal concentrations for synergy were 0.25–100 nM C5a and 40–500 nM UDP, whereas for BMDM they were 0.1–3 nM C5a and 150–500 nM UDP.

Synergy Is Dependent on Signaling through Both Gα$_i$- and Gα$_q$-dependent GPCRs—C5a engages C5aR, which signals predominantly through Gα$_i$-coupled heterotrimers (11, 25, 26). Thus, in BMDM and RAW264.7, the Ca^{2+} response to C5a was inhibited following treatment with pertussis toxin (PTX), whereas that of UDP was not (Fig. 2*A* and supplemental Fig. S1). PTX-mediated inhibition of signaling by low concentrations of C5a (<1 nM) was complete, but at high concentrations residual PTX-insensitive calcium signaling was detected both in WT BMDM and in BMDM from mice lacking either Gα$_q$ or Gα$_{11}$ (data not shown). Saturation of PTX intoxication of the C5a Ca^{2+} response was reached using 5 ng/ml for 18 h (supplemental Fig. S1). Others have demonstrated a role for Gα$_{15}$ in C5a signaling in primary macrophages (27). Although our data indicate that most C5a signaling is PTX-sensitive, they are consistent with some signaling through Gα$_{15}$ when C5a is present in high concentrations. The Ca^{2+} response to C5a in BMDM from
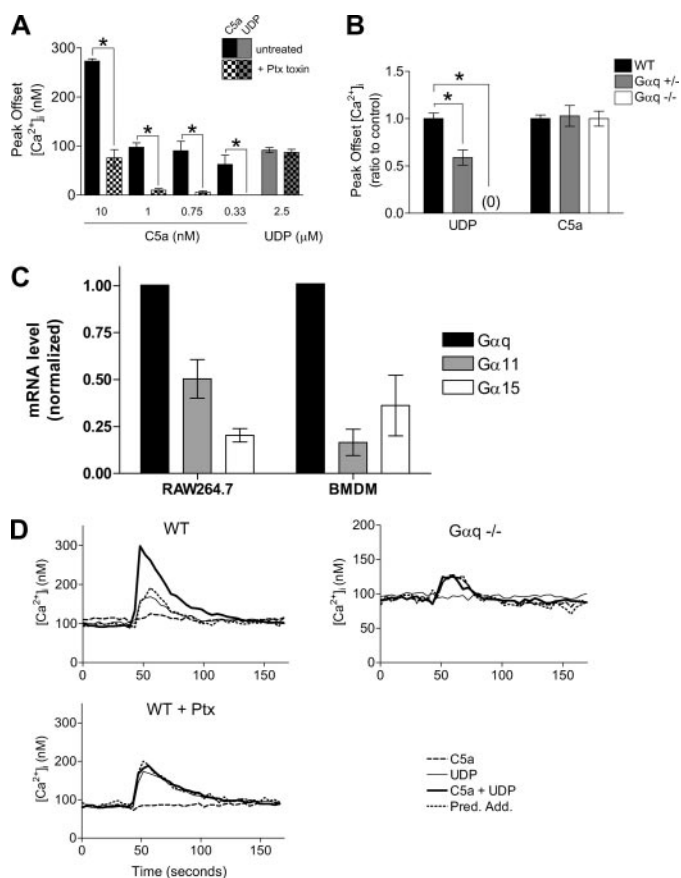
FIGURE 2. **Synergy requires Gα_q- and Gα_i-heterotrimer subunit effectors.** Intracellular Ca²⁺ responses were measured in Fura2-loaded BMDMs. *A*, C5a Ca²⁺ responses are mostly PTX sensitive. BMDM cultured overnight with or without PTX (100 ng/ml) were stimulated with different concentrations of C5a (0.33 to 10 nM), or a single concentration of UDP (2.5 μM), and the peak offset of the Ca²⁺ responses was determined. Shown is a representative experiment of seven with similar results. Values are mean ± S.E. of three to four replicate samples per condition. *, $p < 0.01$. *B*, UDP responses are Gα_q-dependent. Wild type (WT), Gα_q heterozygote (+/−), and Gα_q-deficient (−/−) BMDM were stimulated with either UDP (2.5 μM) or C5a (10 nM). Peak offsets of responses are shown normalized to those of the wild-type cells from each experiment. Values are mean ± S.E. from three experiments. *, $p < 0.001$. *C*, quantitative reverse transcriptase-PCR for Gα_q family isoforms q, 11, and 15 was performed on RAW264.7 cell and BMDM samples to determine relative prevalence. Transcript levels were normalized to those for Gα_q for the same cell type. Data shown are mean ± S.E. from $n = 3$ samples per cell. *D*, synergy following dual ligand stimulation requires both Gα_q and Gα_i subunits. WT or Gα_q-deficient (−/−) BMDM were stimulated with UDP (500 nM), C5a (0.75 nM), or simultaneous UDP and C5a. WT cells were cultured overnight with or without PTX (100 ng/ml). Data shown are from a representative experiment of three to four with similar results. Each line in the graphs represents the average of three to four individual wells in the assay.

mice genetically deficient in Gα_{i2} was intact (data not shown), suggesting that Gα_{i3} is sufficient to support C5a signaling in these cells, because Gα_{i1} and G$_o$ are not expressed in macrophages (data not shown). Inhibition by PTX was similar to that observed for WT cells (data not shown).

UDP binds to purinergic receptors of the P2Y family, which usually signal through members of the Gα_q family (12, 28, 29). In accord with this, we found that the Ca²⁺ response was completely lost in BMDM from Gα_q-deficient mice (Fig. 2*B*). Surprisingly, although BMDM express other members of the Gα_q family, including Gα_{11} and Gα_{15} (Fig. 2*C*), these are evidently unable to substitute for Gα_q in response to UDP. Furthermore, the BMDM from Gα_{11}-deficient mice had no reduction in Ca²⁺

responses for UDP (or for C5a, data not shown) compared with wild type.

UDP only binds with high affinity to the P2Y6 receptor on macrophages. UTP, which has much lower affinity for P2Y6, binds also to P2Y2 and P2Y4 receptors (12, 28). To demonstrate that the responses to UDP did not involve contaminating UTP, we separately tested UTP and UDP before and after treatment with hexokinase (12), which catalyzes conversion of UTP to UDP. Hexokinase treatment of UDP had no effect on its capacity to increase [Ca²⁺]$_i$ in BMDM (not shown), indicating that contaminating UTP was not responsible for the observed responses in BMDM. The efficacy of hexokinase treatment was confirmed by showing that hexokinase treatment of UTP ablated its capacity to increase [Ca²⁺]$_i$ in NIH 3T3 cells, which respond to UTP but not UDP.

The removal of either Gα_q or Gα_i, via genetic deletion or PTX intoxication, respectively, also eliminated any synergistic Ca²⁺ response to dual ligand stimulation (Fig. 2*D*). Thus, synergy between C5a and UDP is dependent on the G$_i$- and G$_q$-linked subunit effectors that are activated by C5a and P2Y6 receptors, respectively.

LPA and PAF Also Synergize with C5a for Ca²⁺ Responses—To determine whether synergy for Ca²⁺ signaling occurred with other ligand pairs, we also examined responses to C5a or UDP in combination with PAF or LPA, both of which induce a Ca²⁺ response in macrophages through GPCRs. Pairing of C5a with either PAF or LPA demonstrated a robust synergy in Ca²⁺ signaling. Little or no synergy was seen with UDP/PAF, UDP/LPA, or PAF/LPA (data not shown). The levels of synergy observed for C5a paired with LPA or PAF (Fig. 3, *A* and *B*) were comparable with those for C5a paired with UDP.

PAF and LPA, like UDP, signaled Ca²⁺ primarily through Gα_q in BMDM (Fig. 3*C*), but unlike UDP this was not exclusive; in the Gα_q-deficient cells residual Ca²⁺ responses for PAF were abrogated by PTX, indicating a minor contribution from Gα_i-coupled pathways. PTX did not reduce the Ca²⁺ response to LPA, but instead surprisingly enhanced it in both Gα_q-deficient and WT BMDM (Fig. 3*D*). These data suggest for the first time that Gα_i-coupled receptors basally inhibit LPA Ca²⁺ signaling. As with UDP, synergy by either LPA or PAF with C5a was lost in Gα_q-deficient BMDM (data not shown). Thus, although these receptors can activate some Ca²⁺ signaling independently of Gα_q, synergy with C5a nonetheless requires Gα_q activation.

Overall, these results indicate that the simultaneous activation of Gα_q and Gα_i heterotrimers results in a synergistic Ca²⁺ response in macrophages. C5aR was the only endogenous Gα_i-coupled GPCR on BMDM that we found to be capable of generating a robust Ca²⁺ response independently, and it was also the only receptor that synergized with ligands for Gα_q-coupled receptors.

Synergy Requires Dual Receptor Occupancy—We next examined the possibility that one ligand might prime cells for subsequent responses, for example, by increasing the supply of PIP$_2$ to provide a heightened state of responsiveness to the second stimulus (30). Although synergy was greatest when C5a and UDP were added simultaneously, it was also evident when ligands were added as much as 10 min apart. The sequence of addition was irrelevant. Fig. 4*A* shows the results for ligands
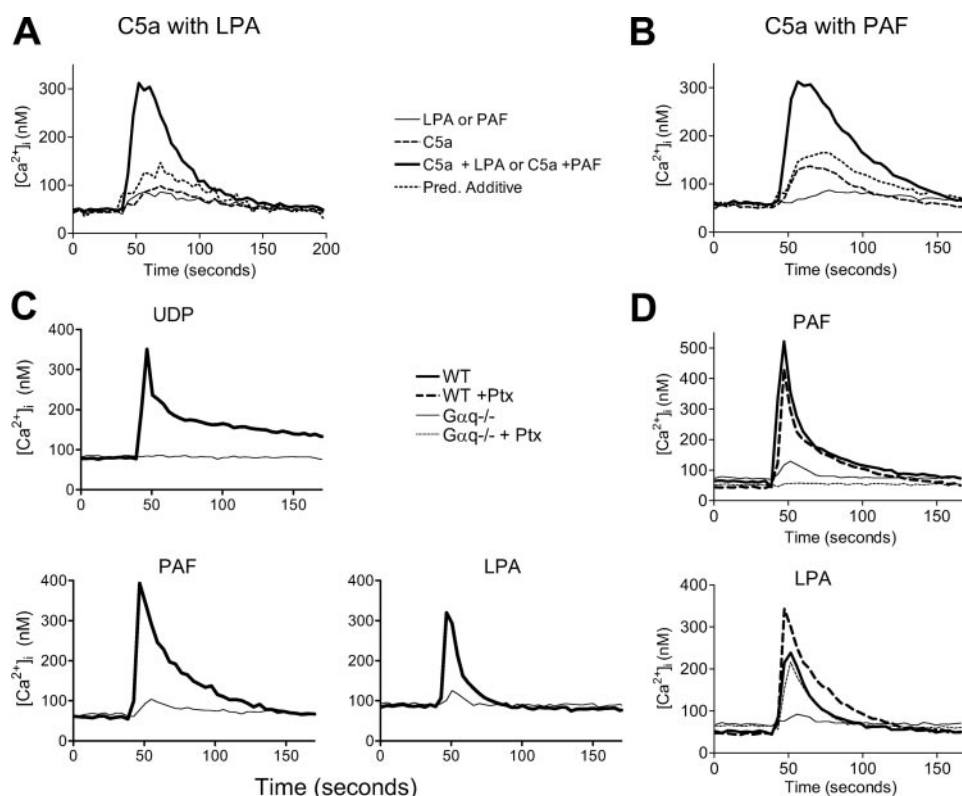
FIGURE 3. **LPA and PAF also show synergy with C5a in Ca^{2+} responses, and they couple mainly with Gα$_q$.** Intracellular Ca^{2+} responses were measured in Fura2-loaded BMDMs. Each line in the graphs represents the average of three to four individual wells per assay. *A*, BMDM were stimulated with C5a (0.25 nM), LPA (0.25 nM), or simultaneous C5a and LPA. Data shown are from a representative experiment of $n = 18$ with similar results. *B*, BMDM were stimulated with C5a (0.25 nM), PAF (0.3 nM), or simultaneous C5a and PAF. Data shown are from a representative experiment of $n = 17$ with similar results. *C*, WT or Gα$_q$(−/−) BMDM were stimulated with UDP (10 μM), PAF (12.5 nM), or LPA (2.5 μM). Data shown are from a representative experiment of $n = 8$–14 with similar results. *D*, WT or Gα$_q$(−/−) BMDM were cultured overnight with or without PTX and then stimulated with PAF (12.5 nM) or LPA (2.5 μM). Data shown are from a representative experiment of four to five with similar results.

at the level of PLCβ activation. Levels of IP$_3$ measured at 30 s and 1 min after ligand additions were increased. Ca^{2+} levels began to decline while IP$_3$ was still rising, indicating that levels of [Ca^{2+}]$_i$ are not solely regulated by levels of IP$_3$.
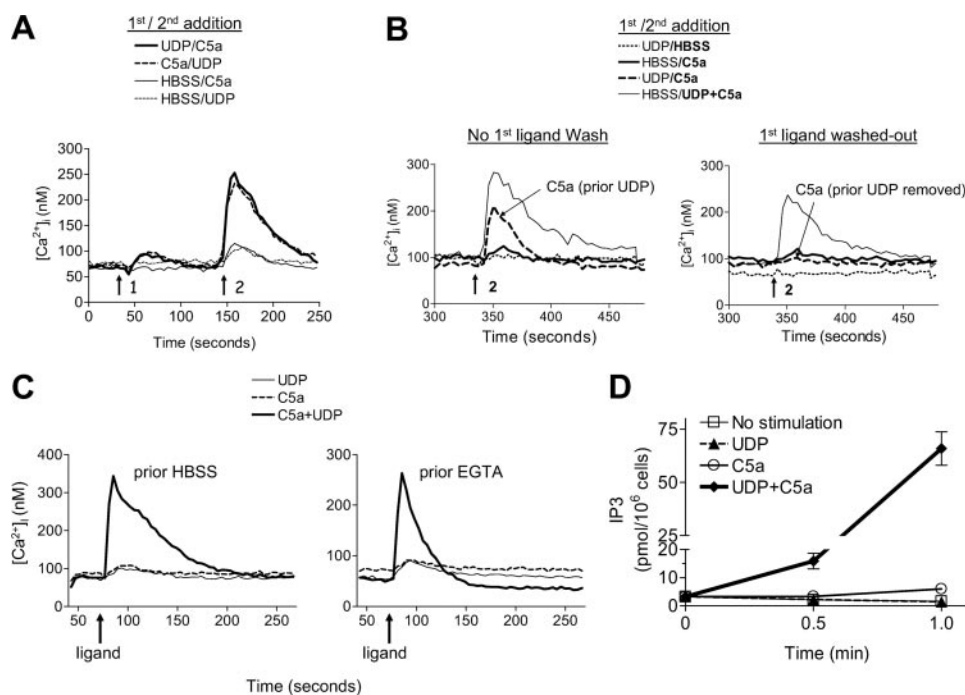
The Synergistic Ca^{2+} Response Is Independent of Feedback Pathways Involving PI 3-Kinase (PI3K) or PKC—Downstream of GPCR activation, PLCβ may be regulated by other signaling components, including those generated following the activation of PI3K (by Gβγ subunits) or PKC (by diacylglycerol) (5). In our studies, however, inhibition of PI3K by LY294002 or PKC by Calphostin C or staurosporine did not significantly affect synergy (supplemental Fig. S2.). The activity of the inhibitors was confirmed by inhibition of Akt or myristoylated alanine-rich c-kinase substrate (MARCKS) phosphorylation (supplemental Fig. S3). These data are further evidence that an early signaling event is involved in the mechanism of synergy.

*C5a and UDP Make Selective Use of PLCβ Isoforms*—To examine the role of PLCβ in the signaling response to C5a and UDP, we first determined levels of transcripts for PLCβ isoforms in RAW264.7 cells and BMDMs. By both microarray analysis (data not shown) and reverse transcriptase-PCR (Fig. 5), we found that both cell types express PLCβ2, PLCβ3, and PLCβ4, with little or no PLCβ1. At the transcript level, the proportions of these PLCβ isoforms, however, differ between RAW264.7 cells and BMDM; normalized to PLCβ3, RAW264.7 cells express similar levels of transcripts for PLCβ2, PLCβ3, and PLCβ4, whereas BMDM express PLCβ2 > PLCβ3 > PLCβ4.

To determine whether C5a and/or UDP made selective use of these PLCβ isoforms, we examined the Ca^{2+} response in BMDM from mice genetically deficient in PLCβ2, PLCβ3, or PLCβ4. BMDM from mice deficient in PLCβ3 demonstrated a marked loss of signaling in response to all GPCR ligands, including, C5a, UDP, PAF, and LPA (Fig. 6 and Table 1). Activation of Ca^{2+} responses, however, was intact in response to ligation of FcγRI by cross-linked IgG$_{2a}$ (Fig. 6), demonstrating that macrophages from PLCβ3-deficient mice are not deficient in the generation of [Ca^{2+}]$_i$ to a non-GPCR ligand. In BMDM from mice deficient in PLCβ4, the Ca^{2+} response to UDP was also consistently reduced, whereas the response to C5a was slightly elevated (Table 1 and Fig. 6) and FcγRI signaling was normal. No loss of signaling to either UDP or C5a was seen in BMDM from mice deficient in PLCβ2. Thus, in BMDM, signaling

separated by 100 s. However, removal of the first ligand during the interim eliminated synergy (Fig. 4*B*). Thus, if either ligand primes the synergistic response, this effect is rapidly lost. Functionally, synergy requires simultaneous receptor occupancy by both ligands.

Synergy Affects the Initial Release of Ca^{2+} from Intracellular Stores and IP$_3$ Production—Synergy between C5a and UDP affected the early rise in [Ca^{2+}]$_i$, suggesting an effect on the release of intracellular calcium stores. To test this, the Ca^{2+} responses to C5a and UDP, either alone or in combination, were measured after acute addition of EGTA to deplete extracellular Ca^{2+}. Synergy occurred in the presence of EGTA, confirming an effect on the release of intracellular Ca^{2+} (Fig. 4*C*). Without EGTA, however, synergy also extended to the sustained phase response, which is dependent on the influx of extracellular Ca^{2+}. Thus, synergy between C5a and UDP begins with the release of intracellular Ca^{2+} stores but extends to the influx of extracellular Ca^{2+}.

The release of Ca^{2+} from intracellular stores is activated by IP$_3$ binding to IP$_3$ receptors on the endoplasmic reticulum to open ER calcium channels (1). Simultaneous stimulation of BMDM with C5a and UDP in amounts that produced a synergistic Ca^{2+} response also resulted in synergy in the production of IP$_3$ (Fig. 4*D*), suggesting synergistic mechanisms are manifest

FIGURE 4. **C5a and UDP produce synergistic Ca²⁺ responses when added serially, but synergy requires dual ligand receptor occupancy.** Intracellular Ca²⁺ responses were measured in Fura2-loaded BMDM. Each line in the graphs represents the average of three to four individual wells per assay. *A*, serial addition of stimuli to BMDM provides synergy. C5a (0.75 nM), UDP (500 nM) or Hanks' balanced salt solution (*HBSS*) were added at the first time point (*arrow 1*), and after a 100-s delay UDP or C5a were added at the second time point (*arrow 2*). The first stimulus was not removed prior to addition of the second. *B*, serial stimulation of BMDM does not provide synergy if the first ligand is removed prior to addition of the second. Either UDP (500 nM) or Hanks' balanced salt solution was added to the cells and incubated for 2 min. The buffer was then left in the wells another 3 min or the buffer was removed, the cells washed, and fresh buffer replaced in the wells. C5a (0.75 nM), C5a + UDP (0.75 nM + 500 nM), or Hanks' balanced salt solution were then added to the wells (2nd addition, *arrow* labeled 2, 5-min delay from 1st addition, thus 3-min delay after 1st ligand removal for washed samples), and the results of the second response period are shown. The *left panel* depicts responses to the 2nd stimulus when the first ligand remains. The *right panel* depicts responses to the 2nd ligand in the absence of the 1st ligand. *C*, synergy was observed in the release of Ca²⁺ from intracellular stores. Each line in the graphs represents the average of three to four individual wells per assay. Hanks' balanced salt solution or EGTA (2 mM) were added to assay wells 30 s prior to C5a (0.75 nM), UDP (500 nM), or simultaneous addition of C5a and UDP. *D*, IP₃ responses of BMDMs. Cells were stimulated with C5a (10 nM), UDP (2.5 μM), or simultaneous C5a and UDP for 0, 30 s, or 1 min and signaling was stopped by cell lysis in perchloric acid as described for IP₃ measurements. IP₃ was measured using a competitive binding assay for the IP₃ receptor and results are reported as picomole/10⁶ cells. Values shown are mean ± S.E. from *n* = 5–10 samples per condition.
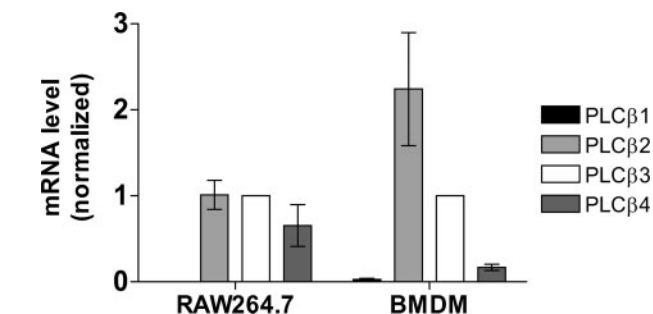
FIGURE 5. **Selective use of the PLCβ3 and -β4 isoforms in GPCR signaling in BMDM did not correlate with higher levels of expression.** Quantitative reverse transcriptase-PCR for PLCβ isoforms 1, 2, 3, and 4 was performed on RAW264.7 cell and BMDM samples to determine relative prevalence. Transcript levels were normalized to those for PLCβ3 for the same cell type. Data shown are mean ± S.E. from *n* = three to four samples per cell. Little to no expression of PLCβ1 mRNA was observed, as shown.

by both C5a and UDP is selectively dependent on PLCβ3, but signaling by UDP is also partly dependent on PLCβ4.

To examine the role of PLCβ in RAW264.7 cells, we used RNAi against the different PLCβ isoforms. The loss of PLCβ

isoforms in response to RNAi was incomplete (supplemental Fig. S4), but this approach allowed the testing of a uniform cell line, and it avoided possible developmental effects on macrophages due to PLCβ isoform loss. The depletion of PLCβ3 from RAW264.7 cells by RNAi reduced signaling by C5a, although not to the same extent as in BMDM genetically deficient in PLCβ3 (Table 2). Cells depleted of PLCβ3 by RNAi were not deficient in their response to UDP, but RNAi against PLCβ4 caused a loss of signaling in response to UDP, with a slight elevation in C5a signaling (Table 2). Thus, signaling by C5a depends mostly on PLCβ3 in both BMDM and RAW264.7 cells. Signaling by UDP is partially dependent on PLCβ3 in BMDM, but we could not detect this dependence in RAW264.7 cells by RNAi of PLCβ3. Signaling by UDP is also dependent on PLCβ4 in both BMDM and RAW264.7 cells, whereas deficiency of PLCβ4 augments C5a signaling in both cells.

Ca²⁺ Responses Are Restored in PLCβ3-deficient BMDM Reconstituted with PLCβ3—Retroviruses were used to transduce wild-type and PLCβ3-deficient BMDM with either YFP-tagged murine PLCβ3 or control YFP-tagged FLAG cDNAs. Single-cell calcium assays were performed, which allowed identification of transduced cells by YFP fluorescence and comparison of responses by transduced and non-transduced cells (Fig. 6, *B* and *C*). Reconstitution of PLCβ3-deficient BMDM with PLCβ3 reconstituted the Ca²⁺ response to both C5a and UDP, alone and in combination, indicating that the loss of Ca²⁺ response in the PLCβ3-deficient cells is not due to an associated developmental defect.

Synergistic Ca²⁺ Responses Also Show Isoform Dependence—We next tested the role of the PLCβ isoforms in synergy between C5a and UDP. In BMDM lacking PLCβ3 or PLCβ4, only those deficient in PLCβ3 were deficient in synergy (Fig. 7*A* and Table 3), as reflected by a reduced synergy ratio. Because signaling by individual ligands was lower than wild type in these cells, the predicted additive responses were also lower, but a residual synergistic response was still detected in PLCβ3-deficient cells (Table 3). Thus synergy in Ca²⁺ signaling, like signaling by individual ligands, is primarily dependent on PLCβ3, but some synergy can be seen without it, Notably, lack of PLCβ4 did not reduce synergy in BMDM but instead enhanced it. We conclude that PLCβ3, but not PLCβ4, plays an important role in synergy between these ligands as well as in their individual responses.
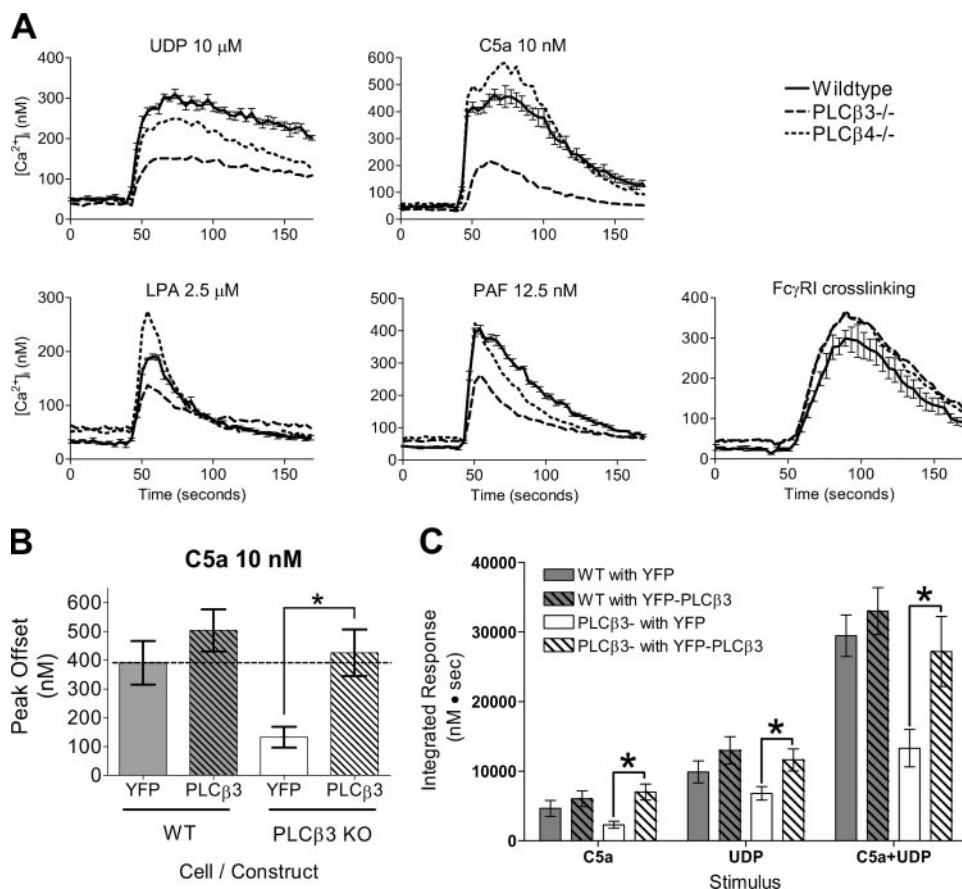
FIGURE 6. **PLCβ isoform dependence of Ca²⁺ responses.** *A*, Ca²⁺ responses for C5a, UDP, LPA, and PAF are reduced in PLCβ3-deficient BMDM compared with wild type, but only the UDP response is reduced in PLCβ4-deficient BMDM. Intracellular Ca²⁺ responses were measured in Fura2-loaded BMDM. Cells were stimulated with near-maximal doses of the 4 ligands tested: C5a (10 nM), UDP (10 μM), LPA (2.5 μM), or PAF (12.5 nM), or by FcγR cross-linking (cells preloaded with 5 μg/ml IgG$_{2a}$, then treated with 44 μg/ml F(ab')$_2$ antibody fragments of rabbit anti-mIgG). Each line in the graphs represents the average of three to four individual wells per assay. Representative experiments are shown for matched wild-type *versus* PLCβ3- or PLCβ4-deficient (−/−) cells from *n* = 8–33 assays with similar results. Assays were performed on 12 PLCβ3-deficient and 4 PLCβ4-deficient BMDM cultures that were independently derived. *B*, expression of PLCβ3 in PLCβ3-deficient BMDM restores single-ligand Ca²⁺ responses. Single cell Ca²⁺ assays were performed on WT or PLCβ3-deficient BMDM transduced with retrovirus encoding YFP-FLAG or YFP-PLCβ3. Cells were stimulated with C5a (10 nM) and peak offset features of the Ca²⁺ traces calculated. Responses by transduced cells were measured in multiple assays of each of two independent batches of infected BMDM. Values shown are mean ± S.E. from *n* = 3–9 samples per condition. *, *p* < 0.05. *C*, expression of PLCβ3 in PLCβ3-deficient BMDM restores dual ligand Ca²⁺ responses to levels observed in WT BMDM. Single cell Ca²⁺ assays were performed on WT or PLCβ3-deficient BMDM transduced with retrovirus encoding YFP-FLAG or YFP-PLCβ3. Cells were stimulated with C5a (0.75 nM), UDP (500 nM), or C5a + UDP, and the Ca²⁺ responses were measured by integration over 2.5 min. Responses by transduced cells were measured in multiple assays of each of three independent batches of infected BMDM. Values shown are mean ± S.E. from *n* = 11–17 samples per condition. *, *p* < 0.05.

homology domain to PIP$_3$ produced by PI3K at the cell membrane. In BMDM, C5a rapidly activated PI3K, with peak phosphorylation of Akt at ~3 min (data not shown). In contrast, UDP did not activate PI3K, and it inhibited the phospho-Akt response to C5a (Fig. 8). This inhibition of Akt phosphorylation by UDP was at least partially selective, as ERK phosphorylation showed additivity. UDP did not inhibit PI3K activation in response to cross-linking of FcγRI (data not shown), demonstrating that signaling by UDP did not globally interfere with all forms of PI3K activation. The observation that UDP inhibits PI3K activation by C5a while promoting Ca²⁺ signaling suggests that these pathways are differentially regulated.

The Opposing Effects of C5a/UDP Signal Interactions on PLC and PI3K Are Reflected in Macropinocytosis—Macropinocytosis, the endocytic process whereby cells internalize substantial volumes of extracellular fluid and solutes, is dependent on both PLC and PI3K (35, 36), and this "sampling" of the environment contributes to macrophage antigen presentation (37, 38). We found that C5a activates macropinocytosis by BMDM, whereas UDP does not. Macropinocytosis was inhibited by dual ligand stimulation (Fig. 9), in contrast to synergy for PLC and Ca²⁺ but in parallel with the inhibition of PI3K.

DISCUSSION

Our studies demonstrate the preferential use of PLCβ isoforms by GPCRs in eliciting a Ca²⁺ response in macrophages. Furthermore, they indicate that synergy in signaling by the Gα$_i$-coupled C5aR, together with the Gα$_q$-coupled P2Y6 receptor for UDP, depends on a selective use of PLCβ3. Synergy in the Ca²⁺ response to C5a and UDP correlated with synergy in IP$_3$ production, suggesting signal convergence at the level of PLCβ activation. In contrast to Ca²⁺ activation, synergy between C5a and UDP was not observed in PI3K activation. Instead, the activation of PI3K by C5a was opposed by UDP. A similar effect was seen in the activation of macropinocytosis, which is dependent on both PLC and PI3K. Thus, synergy was selective for IP$_3$ production and Ca²⁺ response, consistent with a selective effect on PLCβ.

The preferential use of PLC isoforms by GPCRs in macrophages did not simply reflect differential levels of expression of

As with Ca²⁺ signaling, BMDM lacking PLCβ3, but not PLCβ4, failed to demonstrate synergy in the production of IP$_3$ (Fig. 7*B*). Thus, studies of both Ca²⁺ and IP$_3$ indicate that synergy in signaling by C5a and UDP is the result of enhanced activity of PLCβ3.

Dual-Ligand Effects on PI 3-Kinase Contrast to Those on PLC—To determine whether the synergistic effects of C5a plus UDP dual ligand stimulation were reflected in signaling events other than PLC activation, we examined activation of PI3K. Gβγ subunits directly activate PI3K-p110γ (31) and GPCRs can also activate PI3K-p110α and PI3K-p110β (32). The Gα$_q$ subunit does not activate PI3K, but instead can interact with and inhibit PI3K-p110α (33, 34). Thus, PI3K activity reflects important proximal GPCR signals. To assess activation of PI3K, we measured the phosphorylation of Akt, which requires anchoring of its pleckstrin

TABLE 1

Single-ligand Ca²⁺ responses in PLCβ isotype-deficient BMDM

BMDMs derived from four to seven individual PLCβ-deficient (−/−) mice per isoform were subjected to Ca²⁺ assays for near maximal concentrations of several GPCR ligands: C5a (10 nM), UDP (2.5 μM), LPA (2.5 μM), and PAF (12.5 nM). Three to four assays per cell population and ligand were performed with three to four replicate samples per assay. Responses were normalized to the matched WT BMDMs in each assay and the table reports the average response of each isotype −/− as % of WT response. Values are shown for peak-offset and integration to 60-s measurements of the Ca²⁺ responses. PLCβ3-deficient BMDM showed reduced responsiveness to four GPCR ligands but not following ligation of FcγRI (FCG). PLCβ4-deficient BMDM showed a reduced Ca²⁺ response phenotype for UDP only.

Measure of response	Ligand	BMDM			
		WT	PLCβ2−/−	PLCβ3−/−	PLCβ4−/−
Peak offset	C5a	100	118 ± 19	20 ± 4[a]	104 ± 6
	UDP	100	150 ± 32	44 ± 3[a]	81 ± 6[b]
	LPA	100	109 ± 13	24 ± 4[a]	86 ± 13
	PAF	100	136 ± 4[b]	38 ± 4[a]	94 ± 3
	FCG	100	114 ± 12	104 ± 10	87 ± 20
Integrated 60s	C5a	100	131 ± 28	18 ± 3[a]	105 ± 5
	UDP	100	159 ± 40	44 ± 3[a]	73 ± 6[b]
	LPA	100	98 ± 10	28 ± 5[a]	89 ± 13
	PAF	100	142 ± 9[b]	34 ± 3[a]	94 ± 9

[a] $p < 0.005$.
[b] $p < 0.05$.

TABLE 2

RNAi against PLCβ3 and PLCβ4 in RAW264.7 reduces Ca²⁺ responses to C5a and UDP respectively

RNAi against PLCβ isoforms in RAW264.7 cells was performed by lentiviral-mediated RNAi using shRNA encoding constructs. Control lines lacking only shRNA were prepared and analyzed in parallel with each RNAi line. Ca²⁺ assays were performed with C5a (30 nM) and UDP (25 μM) and responses were quantified by peak offset and integration to 1 or 2.5 min after ligand addition. Values were normalized to responses of control lines in each assay, and results of replicate lines were pooled to present the average response as a percent of control. Results represent 2–5 lines per target with three to four assays per line and three to four samples per ligand per assay.

| RNAi target	No. lines	C5a			UDP		
		Peak offset	Intgrated 1 m	Integrated 2.5 m	Peak offset	Intgrated 1 m	Integrated 2.5 m
PLCβ2	2	71	58	82[a]	104	78	104
PLCβ3	2	61[b]	46[b]	62[b]	107	110	111
PLCβ4	5	125[a]	115	111	97	95	88[b]

[a] $p < 0.01$.
[b] $p < 0.05$.

transcripts for the PLCβ isoforms. Four isoforms of PLCβ have been identified (4). We found that both BMDM and RAW264.7 cells expressed transcripts for PLCβ2, β3, and β4 but not PLCβ1, as determined by gene array analyses on Affymetrix chips and by reverse transcriptase-PCR. We have not been able to develop assays that adequately quantify differences in protein expression of these PLCβ isoforms, but our results, nonetheless, suggest that the selective use of PLCβ3 in macrophages for Ca²⁺ signaling and synergy is despite the expression of PLCβ2 and PLCβ4. Thus, in contrast to platelets and neutrophils, PLCβ3 appears to be the major functional isoform in macrophages. While this article was in preparation, Wang *et al.* (39) also reported reduced Ca²⁺ responsiveness to C5a by macrophages from PLCβ3-deficient mice, and they linked this to increased apoptosis, and diminished atherosclerosis. Our studies demonstrate that in macrophages UDP can use PLCβ4 as well as PLCβ3, but C5a synergizes with UDP and other activators of Gα$_q$ through signals that converge at the level of PLCβ3, and responsiveness can be restored by transduction of cells with PLCβ3, showing that the defect in signaling does not reflect developmental changes in other pathways.
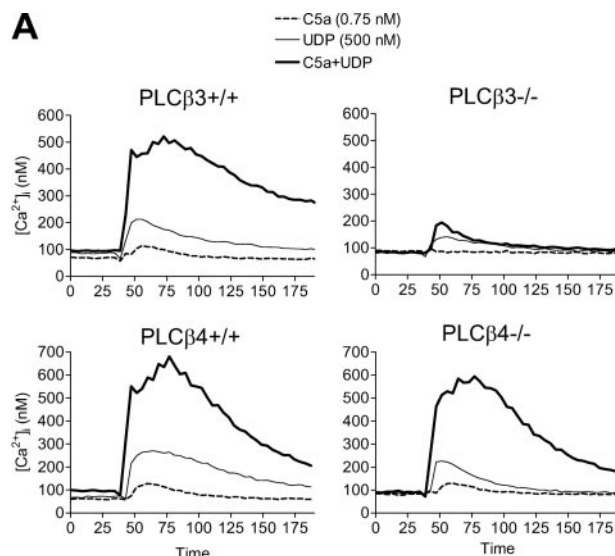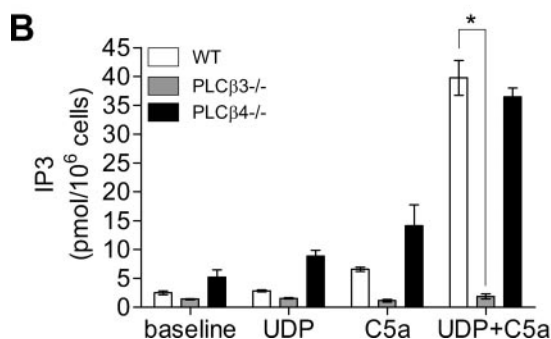
FIGURE 7. **The synergistic Ca²⁺ response shows selective use of the PLCβ3 isoform.** Matched wild-type (+/+) versus PLCβ3- or PLCβ4-deficient (−/−) BMDMs were assayed for their ability to reflect synergistic responses to C5a plus UDP. *A*, intracellular Ca²⁺ responses were measured in Fura2-loaded BMDM. Each line in the graphs represents the average of three to four individual wells per assay. Cells were stimulated with C5a (0.75 nM), UDP (500 nM), or both ligands. Data shown are from representative experiments of $n = 9$–19 with similar results. *B*, IP$_3$ production in PLCβ isoform-deficient BMDM. Cells were stimulated with C5a (10 nM), UDP (2.5 μM), or simultaneous C5a and UDP as indicated, and signaling was stopped by cell lysis at 1 min after stimulation. IP$_3$ was measured using a competitive binding assay for the IP$_3$ receptor, and results are reported as picomole/10⁶ cells. Data represent pooled results from two to four assays with 2 replicate samples per condition per assay. *, $p < 0.005$.

TABLE 3

Ca²⁺ response synergy in PLCβ isotype-deficient BMDMs

BMDMs derived from individual PLCβ isotype-deficient mice were subjected to Ca²⁺ assays for synergy between C5a and UDP (0.75 + 500 nM). Peak offset values from Ca²⁺ assays in Fura2-loaded cells were normalized to corresponding controls in each assay. Data were pooled to report average values as a percent of control (% WT) for the individual ligands and the corresponding predicted additive responses. Synergy observed was reported as a percent of the calculated additive Ca²⁺ response for each cell type. Data were from 6 or 4 independent lines for PLCβ3 or PLCβ4-deficient cells, respectively, with two to four replicate assays per population and three to four samples per condition per assay.

BMDM	C5a[a]	UDP[a]	Calculated additive[a]	Synergy observed[b]
WT	100	100	100	265 ± 33
PLCβ3−/−	25 ± 11[c]	41 ± 5[c]	34 ± 5[c]	158 ± 21[d]
PLCβ4−/−	103 ± 5	61 ± 5[d]	78 ± 6[d]	315 ± 38[d]

[a] Values are expressed as percent WT.
[b] Values are expressed as present of calculated additive.
[c] $p < 0.005$.
[d] $p < 0.05$.

Synergy in the macrophage Ca²⁺ response was observed both in the initial, rapid release of Ca²⁺ from intracellular stores and in the sustained elevation of cytoplasmic Ca²⁺ levels.
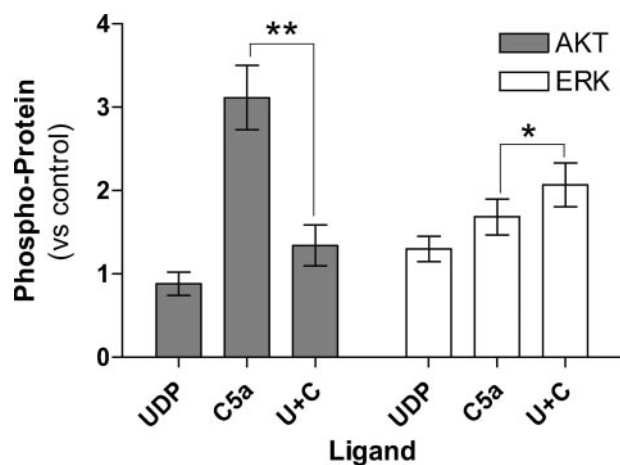
FIGURE 8. UDP and other Gα$_q$-coupled ligands antagonize C5a stimulation of PI 3-kinase. Adherent BMDM were stimulated with C5a (10 nM), UDP (10 μM), LPA (2.5 μM), PAF (50 nM), C5a plus UDP, C5a plus LPA, or C5a plus PAF. After 1 min of stimulation, the assay was stopped by sample lysis. Western blots were probed with specific antibodies and quantified using a phosphorimager. Phosphoprotein values were normalized to levels of Rho-GDI in the samples and then expressed as a -fold increase *above* the baseline level, represented by the average of control cell samples not stimulated with specific ligands. Data are shown for P-Akt and P-ERK from nine replicate experiments as mean ± S.E. *, $p < 0.05$; **, $p < 0.01$.
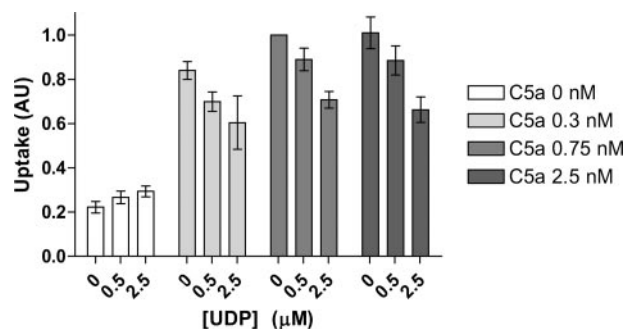
FIGURE 9. UDP inhibits C5a-stimulated macropinocytosis. BMDM were stimulated with or without C5a (0, 0.3, 0.75, and 2.5 nM) in the presence or absence of UDP (0, 0.5, and 2.5 μM) in assays of macropinocytosis. Uptake of extracellular fluorescein isothiocyanate-dextran was assessed by cytometry and normalized to the positive control (C5a 0.75 nM) in each assay (arbitrary units, *AU*) for summary purposes. Values show the mean ± S.E. from eight experiments ($n = 4–8$ per condition).

This observation is important, as there are examples of ligand interactions that increase $[Ca^{2+}]_i$ only via the influx of Ca^{2+} through plasma membrane Ca^{2+} channels (40).

Synergy between Gα$_i$- and Gα$_q$-coupled receptors has previously been observed in other cell types. In several systems, including smooth muscles, astrocytes, and kidney epithelial cells, Gα$_i$-coupled GPCRs may alone not trigger a Ca^{2+} response, but responses may be facilitated in combination with, or after priming by, Gα$_q$-coupled receptors (41–43). This synergy is reflected in the generation of IP$_3$, as in our current studies of macrophages, implicating PLC in the pathway of synergy.

Our findings narrow the possible mechanisms by which synergy in Ca^{2+} signaling by macrophages may occur. All PLCβ isoforms can bind Gα$_q$ subunits, albeit with differing affinities (44–48), and under certain conditions PLCβ4 demonstrates the highest specific activity for hydrolyzing PIP$_2$ (49). Consistent with this, the absence of PLCβ4 reduced mobilization of $[Ca^{2+}]_i$ by all ligands that activate Gα$_q$, including UDP, LPA,

and PAF. The loss of PLCβ4, however, did not impair synergy but instead increased it. Thus, PLCβ4 appears to inhibit rather than promote synergy in macrophages. PLCβ2 and -β3 are both potently activated by Gβγ (25, 47, 50, 51), whereas PLCβ4 is not (49). Although most Ca^{2+} synergy was lost in mice lacking PLCβ3, we could still detect low levels of synergy. We hypothesize that PLCβ2 may be capable of mediating synergy, but in macrophages the contribution of PLCβ2 is small in relation to that of PLCβ3. In all, these results suggest that synergy between C5a and UDP in Ca^{2+} signaling in macrophages does not require multiple isoforms of PLCβ but instead involves the convergence of molecular mechanisms that primarily activate PLCβ3, but which may to a lesser extent activate PLCβ2.

Synergy between the Gα$_i$ receptor C5aR and Gα$_q$ receptors does not establish that Gα$_q$ itself participates in the synergy. Gβγ signaling may differ between C5a and UDP, and synergy could reflect interactions between their unique Gβγ pathways. Indeed, loss of Gβ2 subunits via RNAi disrupts C5a but not UDP Ca^{2+} responses in RAW264.7 cells (Ref. 52, and data not shown).

In our studies, C5a synergized not only with UDP, but also with PAF and LPA in stimulating a rise in $[Ca^{2+}]_i$. Studies of Gα$_q$-deficient BMDM confirmed that both PAF and LPA utilize Gα$_q$, but they also revealed important and interesting differences between these ligands and UDP. Unlike UDP, neither PAF nor LPA was fully dependent on Gα$_q$. The remaining Ca^{2+} signaling with PAF utilized Gα$_i$, as interruption of this pathway with PTX in the absence of Gα$_q$ removed all Ca^{2+} signaling in response to PAF. In contrast, LPA Ca^{2+} signaling was not reduced by PTX. Instead it was markedly increased. The G proteins used by LPA to elevate $[Ca^{2+}]_i$ in Gα$_q$-deficient BMDM are unknown, but it appears that they are normally inhibited by Gα$_i$.

At high ligand concentrations, C5a also demonstrated some PTX-insensitive activation of Ca^{2+} signaling. We found that this response was still present in Gα$_q$- or Gα$_{11}$-deficient mice, suggesting coupling of C5aR to the more promiscuous Gα$_{15}$, as has been observed by others (27). However, no Ca^{2+} synergy was observed with the combination of two Gα$_q$ family-linked ligands. Optimal synergy was observed at low concentrations of C5a, where the C5a-stimulated Ca^{2+} response was entirely PTX sensitive, so we infer that the synergy is attributable to the Gα$_i$ activation by C5aR. In BMDM, the C5a receptor was the only Ca^{2+} signaling receptor identified that was primarily dependent on Gα$_i$.

GPCR-mediated PLCβ activation can be regulated by positive or negative feedback loops. The pleckstrin homology domain of PLCβ preferentially binds to the phosphatidylinositol 3-phosphate product of PI3K (4) and thus PI3K has the potential to modulate PLCβ activity. In our studies, however, inhibition of PI3K by LY294002 did not alter the Ca^{2+} synergy, indicating that PI3K does not measurably contribute to synergy. PKC may interact with PLC at several levels. It can directly phosphorylate PLCβ, inactivating it (53). It can also phosphorylate and regulate signaling via GPCRs, and can phosphorylate some G protein-coupled receptor kinases (54). In our studies, however, inhibition of PKC with either Calphostin C or staurosporine did not alter Ca^{2+} synergy.

The acute nature of the synergy observed (occurring within seconds of dual ligand addition) and the demonstrated requirement for simultaneous dual receptor occupancy argue against the possibility that one receptor might drive "priming" events affecting responses to the second receptor. Mechanisms for synergy reflecting priming effects have been proposed in a number of other systems (55). The immediate synergy in macrophages precludes changes in receptor or other protein expression levels. Alternatively, a priming event could increase the supply of the PLC substrate PIP_2 to enhance production of IP_3 (56–58), and in some cases this has been shown to persist for hours after the first ligand stimulation. This synergy mechanism would not require dual receptor occupation during heterologous ligand stimulations of Ca^{2+} unless increases in the supply of PIP_2 were lost rapidly (we tested 3 min after 1st ligand removal by which time synergy was lost).

The consequences of combined signaling by C5a and UDP in macrophages may be particularly important in areas of inflammation, where C5a is produced, and where UDP may be released from dying cells (59). C5a in particular plays a central role in inflammation, and consequences of Ca^{2+} signaling would be augmented by UDP, whereas consequences of PI3K activation would be inhibited. The recent report describing a reduction of atherosclerosis in PLCβ3-deficient mice, due to macrophage hypersensitivity to apoptotic induction, links inflammatory outcome to Ca^{2+} signaling and survival in macrophages (39).

REFERENCES

1. Berridge, M. J., Bootman, M. D., and Roderick, H. L. (2003) *Nat. Rev. Mol. Cell. Biol.* **4,** 517–529
2. Carafoli, E., Santella, L., Branca, D., and Brini, M. (2001) *Crit. Rev. Biochem. Mol. Biol.* **36,** 107–260
3. Feske, S. (2007) *Nat. Rev. Immunol.* **7,** 690–702
4. Rhee, S. G. (2001) *Annu. Rev. Biochem.* **70,** 281–312
5. Werry, T. D., Wilkinson, G. F., and Willars, G. B. (2003) *Biochem. J.* **374,** 281–296
6. Toms, N. J., and Roberts, P. J. (1999) *Neuropharmacology* **38,** 1511–1517
7. Abrams, C. S. (2005) *Curr. Opin. Hematol.* **12,** 401–405
8. Natarajan, M., Lin, K. M., Hsueh, R. C., Sternweis, P. C., and Ranganathan, R. (2006) *Nat. Cell Biol.* **8,** 571–580
9. Hawlisch, H., Wills-Karp, M., Karp, C. L., and Kohl, J. (2004) *Mol. Immunol.* **41,** 123–131
10. Boeynaems, J. M., and Communi, D. (2006) *J. Investig. Dermatol.* **126,** 943–944
11. Skokowa, J., Ali, S. R., Felda, O., Kumar, V., Konrad, S., Shushakova, N., Schmidt, R. E., Piekorz, R. P., Nurnberg, B., Spicher, K., Birnbaumer, L., Zwirner, J., Claassens, J. W., Verbeek, J. S., van Rooijen, N., Kohl, J., and Gessner, J. E. (2005) *J. Immunol.* **174,** 3041–3050
12. Del Rey, A., Renigunta, V., Dalpke, A. H., Leipziger, J., Matos, J. E., Robaye, B., Zuzarte, M., Kavelaars, A., and Hanley, P. J. (2006) *J. Biol. Chem.* **281,** 35147–35155
13. Hashimoto, K., Watanabe, M., Kurihara, H., Offermanns, S., Jiang, H., Wu, Y., Jun, K., Shin, H. S., Inoue, Y., Wu, D., Simon, M. I., and Kano, M. (2000) *Prog. Brain Res.* **124,** 31–48
14. Offermanns, S., Hashimoto, K., Watanabe, M., Sun, W., Kurihara, H., Thompson, R. F., Inoue, Y., Kano, M., and Simon, M. I. (1997) *Proc. Natl. Acad. Sci. U. S. A.* **94,** 14089–14094
15. Offermanns, S., Zhao, L. P., Gohla, A., Sarosi, I., Simon, M. I., and Wilkie, T. M. (1998) *EMBO J.* **17,** 4304–4312
16. Xie, W., Samoriski, G. M., McLaughlin, J. P., Romoser, V. A., Smrcka, A., Hinkle, P. M., Bidlack, J. M., Gross, R. A., Jiang, H., and Wu, D. (1999) *Proc. Natl. Acad. Sci. U. S. A.* **96,** 10385–10390
17. Jiang, H., Lyubarsky, A., Dodd, R., Vardi, N., Pugh, E., Baylor, D., Simon, M. I., and Wu, D. (1996) *Proc. Natl. Acad. Sci. U. S. A.* **93,** 14598–14601
18. Kano, M., Hashimoto, K., Watanabe, M., Kurihara, H., Offermanns, S., Jiang, H., Wu, Y., Jun, K., Shin, H. S., Inoue, Y., Simon, M. I., and Wu, D. (1998) *Proc. Natl. Acad. Sci. U. S. A.* **95,** 15724–15729
19. Jiang, H., Kuang, Y., Wu, Y., Xie, W., Simon, M. I., and Wu, D. (1997) *Proc. Natl. Acad. Sci. U. S. A.* **94,** 7971–7975
20. Salmon, P., Kindler, V., Ducrey, O., Chapuis, B., Zubler, R. H., and Trono, D. (2000) *Blood* **96,** 3392–3398
21. Rossi, G. R., Mautino, M. R., and Morgan, R. A. (2003) *Hum. Gene Ther.* **14,** 385–391
22. Fraser, I., Liu, W., Rebres, R., Roach, T., Zavzavadjian, J., Santat, L., Liu, J., Wall, E., and Mumby, M. (2006) *Methods Mol. Biol.* **365,** 261–286
23. Morita, S., Kojima, T., and Kitamura, T. (2000) *Gene Ther.* **7,** 1063–1066
24. Grynkiewicz, G., Poenie, M., and Tsien, R. Y. (1985) *J. Biol. Chem.* **260,** 3440–3450
25. Jiang, H., Kuang, Y., Wu, Y., Smrcka, A., Simon, M. I., and Wu, D. (1996) *J. Biol. Chem.* **271,** 13430–13434
26. Sarndahl, E., Bokoch, G. M., Boulay, F., Stendahl, O., and Andersson, T. (1996) *J. Biol. Chem.* **271,** 15267–15271
27. Davignon, I., Catalina, M. D., Smith, D., Montgomery, J., Swantek, J., Croy, J., Siegelman, M., and Wilkie, T. M. (2000) *Mol. Cell. Biol.* **20,** 797–804
28. Di Virgilio, F., Chiozzi, P., Ferrari, D., Falzoni, S., Sanz, J. M., Morelli, A., Torboli, M., Bolognesi, G., and Baricordi, O. R. (2001) *Blood* **97,** 587–600
29. Erb, L., Liao, Z., Seye, C. I., and Weisman, G. A. (2006) *Pflugers Arch.* **452,** 552–562
30. Stephens, L., Jackson, T. R., and Hawkins, P. T. (1993) *Biochem. J.* **296,** 481–488
31. Hazeki, O., Okada, T., Kurosu, H., Takasuga, S., Suzuki, T., and Katada, T. (1998) *Life Sci.* **62,** 1555–1559
32. Thelen, M., and Didichenko, S. A. (1997) *Ann. N. Y. Acad. Sci.* **832,** 368–382
33. Ballou, L. M., Lin, H. Y., Fan, G., Jiang, Y. P., and Lin, R. Z. (2003) *J. Biol. Chem.* **278,** 23472–23479
34. Ballou, L. M., Chattopadhyay, M., Li, Y., Scarlata, S., and Lin, R. Z. (2006) *Biochem. J.* **394,** 557–562
35. Swanson, J. A., and Watts, C. (1995) *Trends Cell Biol.* **5,** 424–428
36. Swanson, J. A., Yirinec, B. D., and Silverstein, S. C. (1985) *J. Cell Biol.* **100,** 851–859
37. Conner, S. D., and Schmid, S. L. (2003) *Nature* **422,** 37–44
38. Rock, K. L., and Shen, L. (2005) *Immunol. Rev.* **207,** 166–183
39. Wang, Z., Liu, B., Wang, P., Dong, X., Fernandez-Hernando, C., Li, Z., Hla, T., Claffey, K., Smith, J. D., and Wu, D. (2008) *J. Clin. Investig.* **118,** 195–204
40. Dianzani, C., Lombardi, G., Collino, M., Ferrara, C., Cassone, M. C., and Fantozzi, R. (2001) *J. Leukocyte Biol.* **69,** 1013–1018
41. Selbie, L. A., and Hill, S. J. (1998) *Trends Pharmacol. Sci.* **19,** 87–93
42. Werry, T. D., Wilkinson, G. F., and Willars, G. B. (2003) *J. Pharmacol. Exp. Ther.* **307,** 661–669
43. Werry, T. D., Christie, M. I., Dainty, I. A., Wilkinson, G. F., and Willars, G. B. (2002) *Br. J. Pharmacol.* **135,** 1199–1208
44. Jiang, H., Wu, D., and Simon, M. I. (1994) *J. Biol. Chem.* **269,** 7593–7596
45. Lee, C. H., Park, D., Wu, D., Rhee, S. G., and Simon, M. I. (1992) *J. Biol. Chem.* **267,** 16044–16047
46. Jhon, D. Y., Lee, H. H., Park, D., Lee, C. W., Lee, K. H., Yoo, O. J., and Rhee, S. G. (1993) *J. Biol. Chem.* **268,** 6654–6661
47. Smrcka, A. V., and Sternweis, P. C. (1993) *J. Biol. Chem.* **268,** 9667–9674
48. Runnels, L. W., and Scarlata, S. F. (1999) *Biochemistry* **38,** 1488–1496
49. Lee, C. W., Lee, K. H., Lee, S. B., Park, D., and Rhee, S. G. (1994) *J. Biol. Chem.* **269,** 25335–25338
50. Wu, D., Katz, A., and Simon, M. I. (1993) *Proc. Natl. Acad. Sci. U. S. A.* **90,**

5297–5301
51. Park, D., Jhon, D. Y., Lee, C. W., Lee, K. H., and Rhee, S. G. (1993) *J. Biol. Chem.* **268,** 4573–4576
52. Hwang, J. I., Fraser, I. D., Choi, S., Qin, X. F., and Simon, M. I (2004) *Proc. Natl. Acad. Sci. U. S. A.* **101,** 488–493
53. Yue, C., Ku, C. Y., Liu, M., Simon, M. I., and Sanborn, B. M. (2000) *J. Biol. Chem.* **275,** 30220–30225
54. Ferguson, S. S. (2001) *Pharmacol. Rev.* **53,** 1–24
55. Yang, C. M., Chien, C. S., Wang, C. C., Hsu, Y. M., Chiu, C. T., Lin, C. C., Luo, S. F., and Hsiao, L. D. (2001) *Biochem. J.* **354,** 439–446

56. Schmidt, M., Lohmann, B., Hammer, K., Haupenthal, S., Nehls, M. V., and Jakobs, K. H. (1998) *Mol. Pharmacol.* **53,** 1139–1148
57. Schmidt, M., Nehls, C., Rumenapp, U., and Jakobs, K. H. (1996) *Mol. Pharmacol.* **50,** 1038–1046
58. Schmidt, M., Bienek, C., Rumenapp, U., Zhang, C., Lummen, G., Jakobs, K. H., Just, I., Aktories, K., Moos, M., and von Eichel-Streiber, C. (1996) *Naunyn-Schmiedeberg's Arch. Pharmacol.* **354,** 87–94
59. Riedemann, N. C., Guo, R. F., Bernacki, K. D., Reuben, J. S., Laudes, I. J., Neff, T. A., Gao, H., Speyer, C., Sarma, V. J., Zetoune, F. S., and Ward, P. A. (2003) *Immunity* **19,** 193–202